The Nature and Morphology of Fissures in Austenitic Stainless Steel Weld Metals

Fissures occur primarily along grain boundaries in the HAZ from the previous weld deposit, and fissuring is enhanced by multiple thermal cycling in the HAZ and is more likely to occur in ferrite-free areas.

BY C. D. LUNDIN AND D. F. SPOND

ABSTRACT. As a result of the testing program to develop the relationship between ferrite and fissuring in Types 308, 308L, 316, 316L, 309, 318, 347 and 16-8-2 austenitic stainless steel weld metals sponsored by the Stainless Steel Advisory Subcommittee of the High Alloys Committee of the Welding Research Council, numerous well documented specimens were available for study. These specimens included those prepared by the 12 industrial laboratories involved in the initial testing and the material deposited in the extension of the original test scheme by the University of Tennessee. Each weld metal was available at four ferrite levels so the effect of ferrite could be readily assessed. Careful study of these specimens by light metallography, scanning electron microscopy and energy dispersive x-ray techniques has revealed information as to the nature and morphology of the fissures present at low ferrite levels.

In essence the study showed:

1. The fissures occur primarily along grain boundaries in the HAZ (i.e., heat-affected zone) of the previously deposited pass.

2. The fissuring tendency is enhanced by multiple thermal cycling in the HAZ.

3. The fissures are invariably more prone to form in ferrite-free areas.

4. The origin of the fissures is related to a liquation mechanism.

5. The size distribution of fissures determined by light metallography at X200 reveals that the average fissure length in Type 308 stainless steel weld metal is 0.004 in. (0.1 mm).

The thermal distribution in the HAZ was determined for the actual welding conditions utilized in the test, and the peak temperature range in which the fissures form is discussed. The influence of weld bead sequence and the effect of multiple thermal cycling on fissuring tendency were evaluated with both SMA deposits and GTA remelting of previously deposited SMA weld metal. The multiple thermal cycle effect can produce a several-fold increase in fissuring propensity and extend the fissuring tendency to higher ferrite levels.

The fissures formed in the weld metals studied do not propagate under room temperature, slow bend conditions even when subjected to 20% plastic strain. The fissures merely open and thus are more easily revealed at low magnifications.

The data obtained in this investigation are compared to the observations and studies by others (unpublished) for service-fabricated, heavy section weldments. It is more than comforting to note that a one-to-one correlation exists between the Fissure Bend Test observations and those recorded from production welds.

C. D. LUNDIN is Section Manager — Welding, Research & Development Division, Babcock & Wilcox Co., Alliance, Ohio, and D. F. SPOND is with AFCO Steel, Little Rock, Arkansas; both authors were with the Chemical and Metallurgical Engineering Dept., University of Tennessee, at the time the program described in this paper was conducted.

Paper presented at the AWS 57th Annual Meeting held in St. Louis, Missouri, during May 10-14, 1976.

Introduction

It is recognized that austenitic stainless steel weld metals are susceptible to fissuring in the fusion zone of single-run beads (Refs. 1-4), in the HAZ (i.e. heat-affected zone) of the base metal (Refs. 1, 5-12), and in the HAZs of weld metal produced by subsequent beads in multipass welds (Refs. 5, 6, 13, 14, 15). The fissuring in single-run welds is normally combated by reduction of weld metal restraint and by composition control to assure residual ferrite in the room temperature microstructure. The base metal HAZ phenomenon has been largely associated with the stabilized grades of stainless such as Type 347 and in recent years has become a relatively minor problem due to improved residual elemental control in the melting and processing of the wrought materials.

Microfissuring in multipass welds in austenitic stainless steels has become of greater importance in recent years due to the increased utilization of heavy section stainless weldments. There is almost universal agreement among investigators that the fissuring in multipass welds is restricted to the weld metal HAZs produced by the multiple weld passes needed to complete a heavy section weldment (Refs. 15, 18, 19, 20, 22-25). It has also been established that composition control of the deposited weld metal, result-

ing in a modest amount of ferrite in the room temperature microstructure, will essentially eliminate the microfissuring tendency. This level of ferrite was more firmly established by Lundin, DeLong and Spond (Ref. 25) in a recent article documenting the ferrite-fissuring tendency of austenitic stainless steel weld metals.

In some studies utilizing actual production weldments of Type 316 stainless steel, the investigators (Refs. 22, 23, 24) did not find any instance of base metal HAZ cracking, nor did they find any microfissures in the last or cover passes in the weld metal. All of the fissures found were within the bulk of the weld metal (buried) in the HAZ of subsequently deposited beads. Literally hundreds of microfissures were observed and fissure densities of up to 70 fissures/in.^{2} (11 fissures/cm^2) were recorded on polished and etched weld sections. Lundin, DeLong and Spond (Ref. 25) also studied fissures in a variety of weld metals in Fissure Bend Test specimens, and their observations confirm those reported for the production weld metals.

Haddrill and Baker (Ref. 15) and Honeycombe and Gooch (Refs. 18, 19, 20) utilized Types 310 and 316 stainless steel weld metals in their work and found, as others had before (Ref. 14), that fully austenitic weld metals are prone to microfissuring. They confirm the observations in the multirun welds (using pad specimens) that the fissuring is relegated to the underlying HAZs and virtually never occurs in passes not subjected to subsequent thermal cycles. Unfortunately, the fissuring of austenitic stainless steel weld metals in multipass heavy section weldments has not been studied extensively to date and much work remains to be done.

Most investigators (Refs. 15, 17, 18, 22-25) writing on the specific nature of the fissures, their location in the microstructure and the mechanism of the fissures agree that:

1. Fissures invariably occur along grain boundaries regardless of whether they are located in the base metal HAZ, weld metal HAZ or in weld beads minimally affected by subsequent weld passes.

2. The fissures are most prone to form in the weld metal HAZs produced by subsequent weld passes.

3. The fissures form at elevated temperatures (above 1600 F or 871 C) and may result from more than one basic (hot cracking) mechanism.

4. Fissuring tendency decreases when the weld metal contains ferrite (room temperature microstructure); and when fissures occur in ferrite-containing weld metals, they form in "ferrite free" areas.

The cause of fissure formation has been studied by several investigators (Refs. 1, 3, 4, 6, 7, 10, 12, 14-18, 20, 21, 26-31) in recent years. Three theories have been presented to explain the mechanism of hot cracking in stainless steels:

1. *Solidification-segregation (Super Solidus) Cracking.* This mode of cracking occurs during the actual deposition of individual weld beads and is related to solute redistribution upon solidification. As indicated above, this mode does not appear to be significant in austenitic stainless steel weld metals because it is not often observed with commercially utilized filler metals.

2. *HAZ Liquation Cracking.* This phenomenon is the basis for most hot cracking theories applied to austenitic stainless steel weld metals. It requires that liquation of low melting segregates, partitioned to grain boundaries, occurs in a given temperature range (usually near the bulk solidus temperature) in concert with a strain of sufficient magnitude to rupture the liquid films.

3. *Ductility-dip Cracking.* This type of cracking results from a loss in ductility occurring over a given temperature range below the bulk solidus (from 1650-1830 F for Type 310 according to Haddrill and Baker (Ref. 15), and around 1560 F and again around 2010 F for Type 347 according to Truman and Kirkby (Ref. 20)). This loss in ductility is sufficient to produce cracking under the influence of welding-induced strains.

Haddrill and Baker (Ref. 15), Shackleton (Ref. 12) and Honeycombe and Gooch (Ref. 18) report that both HAZ liquation and ductility-dip cracking may be operative in the weld metal at the same time. However, Honeycombe and Gooch believe that HAZ liquation is the dominant mechanism while Haddrill and Baker maintain that ductility-dip cracking is more prevalent.

Regardless of the specifics of the mechanism, it can be simply stated that:

1. The material comprising a weldment exhibits a region (degraded microstructure) which possesses a limited capacity to tolerate strain within some critical range of temperature.

2. The strain imposed upon the weldment by the combined action of thermal and restraint conditions within this critical range of temperature exceeds the strain tolerance of the degraded microstructural region.

A degraded microstructural region in austenitic stainless steel weld metal may be solidification segregation related but may not be influential in regard to fissuring until conditioned by the thermal cycles from succeeding passes. After the weld metal has been thermal cycled by subsequent passes, it may be more susceptible to fissuring. In addition, if the matrix is strengthened by a precipitation reaction which is enhanced by subsequent weld cycles, the fissuring tendency may be influenced in that the strains occurring during the subsequent thermal cycles may be forced to occur in and about the degraded microstructural region.

Fig. 1 — Light micrograph of a fissure along a grain boundary near an interpass boundary (see arrow) in a polished and etched sample of Type 316L austenitic stainless steel weld metal (0.5 FN), unbent, transverse section. X100 (reduced 30% on reproduction)

Alternately, it may be the accumulation of strains produced by subsequent thermal cycles which is responsible for cracking. When the strain accumulation is sufficient, rupture or fissuring occurs. It is, however, most likely a number of factors operating together which are ultimately responsible for the type of fissuring observed in austenitic stainless steel weld metals. It is to be this end that the current research has addressed the issue of fissuring in austenitic stainless steel weld metals.

Fissure Morphology in Austenitic Stainless Steel Weld Metals

General

As a result of the testing program to develop the relationship between ferrite and fissuring in Types 308, 308L, 316, 316L, 309, 318, 347, and 16-8-2 austenitic stainless steel weld metals, numerous well documented specimens were available for study (Ref. 25). With the exception of 16-8-2, each weld metal was available at four ferrite levels (approximately OFN, 2FN, 4FN, and 6FN) so that the influence of ferrite on fissure morphology and location could be assessed. The 16-8-2 weld metal was deposited from

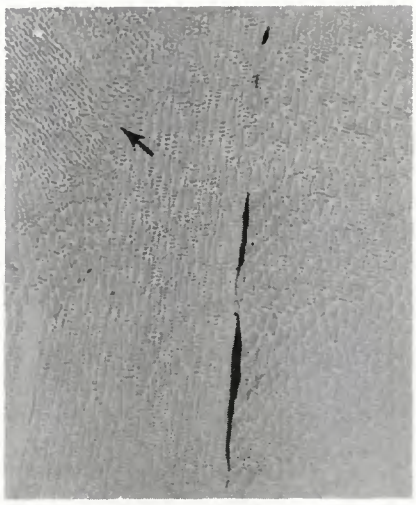

Fig. 2 — Light micrograph of a fissure along a grain boundary near an interpass boundary (see arrow) in a polished and etched sample of Type 309 austenitic stainless steel weld metal (0.4 FN), bent, transverse section. X100 (reduced 29% on reproduction)

Fig. 3 — Light micrograph of a fissure in a ferrite-free area of Type 316 stainless steel weld metal (avg. 2.5 FN), bent, longitudinal, top view secion. X250

two commercial electrode lots of low ferrite level and could not be assessed with regard to its cracking tendency over a ferrite range. The range of ferrite level for each weld metal was obtained by adjustment of the compounding in the electrode coatings. The chemical analyses of the core wires and of the deposited weld metals were presented previously (Ref. 25) and it is to be noted that the trace elements (especially phosphorous and sulphur) are within the range of commercial electrodes.

The aforementioned testing utilized the Fissure Bend Test method (Refs. 25, 32) which employs a multirun, double-layer, weld pad deposited by the SMA process to evaluate fissuring in relatively undiluted weld metal. In this testing scheme the pad surfaces are prepared by milling, grinding or polishing, and then are bent in tension to a 120 deg included angle to expose fissures for detection by fluorescent penetrant inspection and binocular microscopy.

From the well documented welds produced during the testing phase, a number of metallographic and scanning electron microscopy (SEM) samples were removed from as-deposited bent and unbent weld pads to characterize the nature and morphology of the fissures present. The samples were chosen from weld specimens of low ferrite content (0-1 FN) where a high incidence of fissuring was observed and from specimens of higher ferrite content (2-3 FN) where fissuring tendency was significantly reduced. In addition, specimens exhibiting penetrant indications of unusual or unexpected nature were thoroughly examined and documented.

Fissure Appearance and Location

In any discussion concerning planar sections through a discontinuity-containing three-dimensional solid, some knowledge of the volumetric configuration of the discontinuity is necessary to gain a full appreciation for its appearance on a planar surface. For the case of fissures, they should be considered essentially disc-shaped with a circular aspect. Thus any cut through a fissure (except for that which lies in the plane of the fissure and would be quite rare) would be displayed as a "line" on a planar section regardless of the angle of cut. If the fissure has some thickness (separation), however, the more oblique cuts would yield more widely separated faces.

All fissures examined in this investigation, regardless of weld metal type, were located along weld metal grain boundaries in the HAZ of a subsequently deposited bead. For example, Fig. 1, a light micrograph showing a fissure in a polished and etched, transverse, unbent section of a Type 316L stainless steel weld pad (0.5 FN), illustrates that the fissure occurs entirely within the weld metal and is located along a grain boundary. In addition, it is to be noted that the fissure is proximate to an interpass boundary (see arrow) and is in the HAZ of the succeeding weld bead.

Figure 2, a light micrograph of a fissure revealed in a polished and etched, transverse, bent section of Type 309 stainless steel weld metal (0.4 FN), also shows the grain boundary mode of fissuring and the relationship of the fissure to the interpass boundary (see arrow). Note that the fissure in the bent pad shown in Fig. 2 is about the same width as the fissure in the unbent pad shown in Fig. 1. The bending of the weld *per se* does not appear to influence the width of a fissure as long as it is wholly contained within the weld metal remote from a free surface. Thus it appears that fissures are present in as-deposited weld metal in much the same form as in the bent weld pads.

Locations where two or more HAZ's overlap in underlying beads throughout thick section, multipass weldments are prime sites for fissure formation. It will be shown later that weld metal at a location in a weld reheated to a high temperature by two or more subsequently deposited beads (and thus lies in the overlapping HAZ's of those beads), experiences an increased susceptibility to fissuring.

The fissures discussed thus far occurred in weld metal of low ferrite level (less than 1 FN in each case). Most austenitic weld metal types exhibit a general fissuring tendency at this low a ferrite level. With increasing amounts of ferrite in the weld metal, the fissuring tendency quickly diminishes and is eventually eliminated at a ferrite level which may vary from 3 FN to 6 FN depending on the weld metal type. The nature and distribution of ferrite phase varies over this same range. At low ferrite levels the ferrite occurs as discrete particles located at the cellular dendritic substructure boundaries with a dominance for triple point intersections. As the nominal ferrite level is increased, the ferrite tends to progressively occupy more of the cell boundary area until at about 4-7% (Ref. 33) the network becomes continuous throughout the cellular dendritic structure.

A high nominal ferrite content does not ensure uniform distribution throughout the weld metal. Gunia and Ratz (Ref. 34), for example, report that a weld metal having an average of 2.8% ferrite may actually vary in ferrite content from 0.3 to 8.1%. This type of variation in ferrite level was observed and confirmed in many metallographic and SEM samples in the present study and also has been shown by others (Refs. 23, 33, 35,36).

The result of ferrite variation within the microstructure is clearly illustrated by a consideration of data presented in a previous article (Ref. 25) and the micrographs shown in Figures 3 and 4. Figure 3 is a light micrograph showing a fissure in a polished and etched metallographic specimen taken from a bent 316 weld pad (average 2.5 FN). This particular weld pad exhibited two penetrant indications which was considered unusual since the average ferrite level was higher than that determined to be necessary to prevent fissuring in 316 weld metal. One of the indications was identified as a small area of lack of fusion between two weld beads

which was not removed during pad surface preparation. The second indication proved to be the fissure shown in Figure 3. The ferrite in this figure is the dark constituent appearing predominantly along the cellular boundaries on the left and right sides of the micrograph. It is to be noted that the ferrite content in the immediate vicinity of the fissure is significantly lower than that in the surrounding areas.

The occurrence of fissures in ferrite-free areas was also observed in 308L weld metal. It had been previously determined that a ferrite level of approximately 3 FN in 308L weld metal is sufficient to prevent fissuring. However, in one bent weld specimen of 308L with a ferrite level of approximately 4 FN, six closely grouped fissures were found. These fissures were approximately 0.010 to 0.020 in. in length and were all located within 0.20 in. of each other near an interpass boundary. The ferrite level of this general area was recorded to be 4.0 FN when measured with a Magne Gage. Metallographic evaluation of a polished and etched sample taken to include these six fissures revealed that they were located in an essentially ferrite-free area. One of these six fissures discussed above is shown in the light micrograph in Figure 4. From this figure it is clear that the fissure is in an area devoid of ferrite, but high concentrations of ferrite exist in close proximity to the fissure.

The evidence uncovered in this investigation, as illustrated above, shows that fissures can occur in nominally "high" ferrite-containing weld metals, but these fissures are confined to the randomly occurring ferrite-free regions.

Other Discontinuities Detected

During the course of the investigation to determine the ferrite-fissuring relationship in austenitic stainless steel weld metals (Ref. 25), several penetrant indications were found that resulted from discontinuities other than fissures. These indications were originally considered to be fissures, but metallographic and scanning electron microscopy examination later revealed the true nature of the discontinuities.

One type of indication is illustrated in Figs. 5a and 5b, which are light micrographs of the surface of a polished and etched, bent sample of 308L weld metal (2.5 FN). These figures show, at 250X and 500X respectively, tears along cellular intersections where austenite and ferrite exist. The tears were caused by surface grinding during weld pad preparation and they were detectable by fluorescent penetrant testing. Tears such as these occurred in areas of high ferrite content and they did not appear in areas almost wholly austenitic. The observation of these grinding tears in high ferrite areas is in contrast to the occurrence of fissures which generally appear in ferrite-free areas.

Fig. 4 — Light micrograph of a fissure in a ferrite-free area in a polished and etched sample of Type 308L stainless steel weld metal (4.0 FN), bent, longitudinal, top view section. X150

Another penetrant indication originally identified as a fissure was a discontinuity found in a bent 316L weld pad at a ferrite level of 5.6 FN. This discontinuity is shown in a SEM micrograph of the pad surface in Figure 6a and outwardly appears to be a true fissure. However, because it had been determined that a ferrite level of 1.5 FN was sufficient to prevent fissuring in 316L weld metal, an explanation for the occurrence of this "fissure" at a ferrite level 5.6 FN was in order. Thus a metallographic sample containing the "fissure" was removed from the pad and polished and etched in order to determine its true nature. Figure 6b, a SEM micrograph obtained from the polished and etched sample, clearly shows that the discontinuity is, in actuality, a crack in an inclusion within the weld metal. Note that the distribution of ferrite in the cell boundaries of the weld metal surrounding the inclusion is virtually continuous at this ferrite level of 5.6 FN. The crack extends across the inclusion but does not extend into the surrounding weld metal. Thus the discontinuity is not related to fissuring of the weld metal in any manner. Apparently, the crack formed as a result of differential contraction rates during solidification or because the inclusion was unable to deform with the surrounding material during bending. Due to the unusual appearance of the inclusion, microanalysis

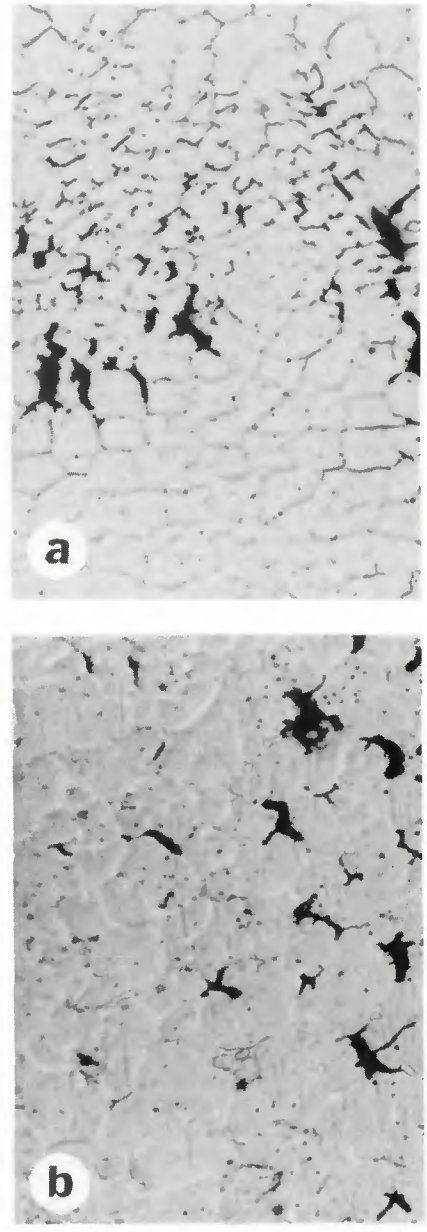

Fig. 5 — Light micrograph of grinding tears in a polished and etched sample of Type 308L stainless steel weld metal (2.5 FN), bent, longitudinal, top view section. (a) — X250; (b) — X500

was performed on various areas (see Figure 6b, areas A, B, and C) by utilizing the energy dispersive x-ray mode of the SEM. The elemental distribution was determined in the three regions shown. Iron, nickel and chromium were found in region A and the analysis of region B yielded iron, nickel, and chromium with a small indication of sulphur. The elements in the center region C were iron and sulphur only. Thus the inclusion was determined to be of a duplex nature with the crack occurring in the center core of FeS.

While the occurrence of the discontinuities discussed above has been observed only in isolated cases, the documentation of their true nature

has proven beneficial because it has been shown that "fissure-like" indications at high ferrite levels in austenitic stainless steel weld metals may be unrelated to the fissuring behavior of the weld metal *per se*. Thus it is not always equitable to disparage the soundness of the weld metal without sufficient investigation and documentation of the occurrence.

Fissure Behavior During Bend Testing

The examination of unbent, surface prepared Fissure Bend Test pads (whether they be milled, ground or metallographically polished and etched) rarely reveals any fissures for most austenitic weld metals. Types 347 and 318 stainless steel weld metals studied here are notable exceptions as these metals exhibited a significant number of fissures on surface ground, unbent pads of low ferrite level. To enhance fissure detection, the test specimen is bent so that the pad surface is subjected to a tensile strain.

In general, for all weld metal types at low ferrite content, the bending operation exposes fissures intersecting or proximate to the pad surface. The number of fissures detected is dependent on many factors including: the weld metal type, the bending strain, the method of surface preparation, the type of microscope utilized, and the magnification at which the pads are examined for fissures (Ref. 32). However, since fissure detection was facilitated by bending, the question of whether the bending operation produced fissures, caused fissures to propagate or elongate, or merely opened the fissures laterally for detection had to be answered. Thus a testing program was initiated to determine:

1. Whether the bending operation produces fissures.

2. The extent of bending strain necessary to expose fissures for detection.

3. Whether fissures extend in length during bending.

To accomplish this task, several Fissure Bend Test pads of Types 308, 316 and 16-8-2 weld metal (all of low ferrite level) were deposited, ground and metallographically polished; and then the pads were examined for fissures. The surfaces were then etched and reexamined. The pads were next subjected to bending in incremental steps and were thoroughly examined after each bending operation. During each examination, particular attention was paid to the interpass boundary region where fissures were expected to be found. Examination of these test specimens at X100 to X200 revealed only two fissures in the unbent pads, one being in a Type 308 specimen and the other in a Type 316 specimen. It was somewhat surprising that so few fissures were found even though the pads were polished, etched and examined at X200.

When each pad was bent to cause a small but perceptible degree of plastic flow ($\simeq$0.4% strain, $\simeq$1 deg bend angle), each was carefully and thoroughly examined and some fissures were found in the Types 308 and 316 stainless steel weld metal. However, for the 16-8-2 weld metal pads about 2% plastic strain ($\simeq$4 deg bend angle) was necessary to initially discover any fissures on the pad surface.

Upon further study it became apparent that the orientation of a fissure with regard to the longitudinal strain applied was the primary condition determining the extent of fissure interface separation. The degree of plastic flow on a microscale as influenced by the orientation of the grains surrounding the fissure location also affects the extent of fissure interface separation. For each weld pad examined, the number of fissures was counted at different degrees of bending, and it was determined that more fissures were found as the bend angle increased or alternately as the extent of straining intensified. To document the phenomenon occurring as bending strain was increased, photomicrography at X200 was carefully and painstakingly performed to unequivocally document the change in fissure appearance. It is to be noted that it was extremely difficult to predetermine the location of fissures in unbent samples even when the microstructure was studied at X500 magnification.

The effect of bending strain on the appearance of a fissure in 316 weld metal (0.4 FN) is illustrated in Figures 7a-7d. Figure 7a is a light micrograph showing the fissure in the weld metal subjected to 0.4% bending strain. The fissure, 0.010 in. in length, is located along a grain boundary and its ends appear well defined. Only a small number of slip bands are evident on the weld metal surface. Figure 7 is a light micrograph showing the same fissure after the weld metal has been subjected to 1% plastic bending strain. The extent of strain at the ends of the fissure is evident from the slip band concentration. By comparison of Figures 7a and 7b, it appears that the fissure increased slightly in length at one end (see small arrow in Figure 7b). However, this small portion of the fissure lies approximately parallel to the direction of bending (see large arrows), and thus the 0.4% plastic bending strain as shown in Figure 7a may have been insufficient to expose this segment of the fissure. Figure 7c is a light micrograph showing the fissure after the weld pad was subjected to 2% plastic strain. The concentration of strain at both ends of the fissure is severe, but it is obvious that the fissure has not propagated. The fissure has widened and it is to be noted that the direction of shift of the fissure walls is in the direction of the applied bending strain (see arrows). Figure 7d is a SEM micrograph of the fissure, taken at a slightly reduced magnification and at a high degree of tilt, after the weld metal was subjected to about 20% plastic bending strain. The fissure has opened but clearly has not increased in length even with this extensive amount of bending strain.

The preceding micrographs are typical of all weld metals tested with regard to the appearance of fissures and the manner in which they open with increasing amounts of bending strain. In only two instances were fissures observed to propagate or interconnect during bending. This occurred only when two fissures were very closely aligned axially (and thus most likely situated along a mutually shared grain boundary). In both instances the amount of weld metal

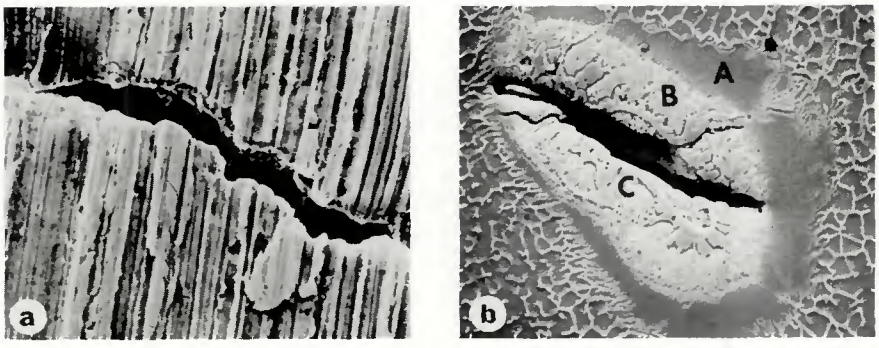

Fig. 6 — SEM micrographs of a discontinuity in a Type 316L stainless steel weld metal pad (5.6 FN), bent, longitudinal, top view section. Left (a) — discontinuity on as-ground pad surface; right (b) — discontinuity on polished and etched surface. X500 (reduced 39% on reproduction)

separating the fissures was small in comparison to the size of the fissures, and the fissures may very well have been interconnected before bending along the grain boundary in the weld metal beneath the plane of examination.

In order to determine if the orientation of the weld beads with regard to the direction of applied strain (longitudinal) in the Fissure Bend Test scheme would alter the location of the fissures or change the extent of fissuring, a study where the beads were deposited transverse to the longitudinal axis of the test specimen was undertaken. This transverse bead sequence yielded the same area for evaluation and about the same length of interpass boundary. There was no difference in location, size or distribution of fissures, and the number of fissures was of the same order as that found in the longitudinal weld beads.

Before leaving the subject of the influence of strain on fissuring, several salient points should be made. As indicated in the introduction, strain invariably plays a part in the fissuring mechanism. Naturally the strains experienced by actual weldments occur over a range of temperatures and are altered as each bead is deposited in a multipass weld.

The level of strain experienced during welding has been the subject of continued research but is fraught with the necessity to deal with high temperatures and their attendant problems in the realm of measurement. However, several investigators have documented the extent of surface strains both transverse and longitudinal to the weld bead. Williams *et al* (Ref. 37) report that the transverse strains are approximately twice as large as the longitudinal strains in austenitic stainless steel welds. For a single weld bead deposited in a groove in thick plate, surface strains of approximately 4% are obtained in the transverse direction. These authors also state that the strains beneath the surface are much higher but naturally defy direct measurement.

Zhitnikov and Zemzin (Ref. 38) report very similar results for austenitic stainless steel, confirming that the strains adjacent to a weld bead are 3-4% as a minimum. They further state that the strains between two closely spaced beads may be twice as high as those occurring along side a single weld bead. Shron (Ref. 39) discussed the triaxiality of strain in thick weldments and relates the strain accumulation in any one zone to the properties of that zone.

The extent of strain through the thickness of a heavy section, multipass weld is not well known but

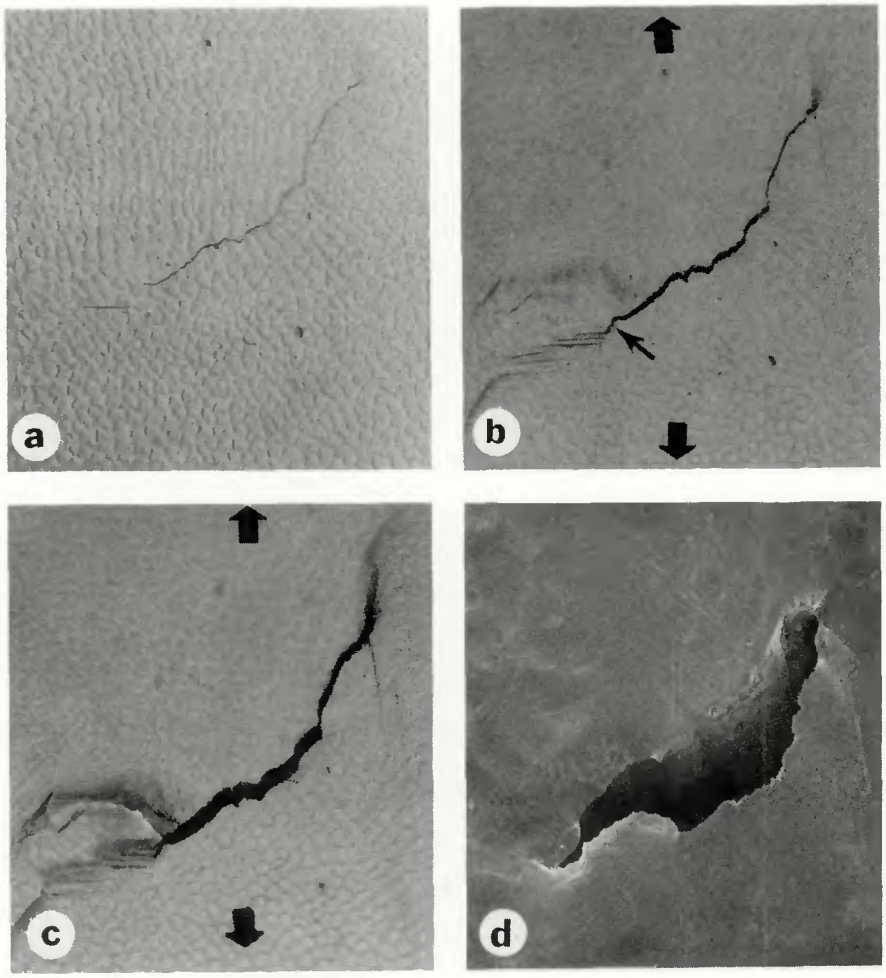

Fig. 7 — Micrographs of a fissure in a polished and etched Type 316 stainless weld metal pad (0.4 FN) as a function of bending strain, longitudinal, top view section. a — Light micrograph, 0.4% plastic strain; X200. b — Light micrograph, 1% plastic strain; X200. c — Light micrograph, 2% plastic strain; X200. d — SEM micrograph, 20% plastic strain; X180 (All micrographs reduced 21% on reproduction)

Table 1 — Average Number of Fissures and Average Fissure Size (Based on Disc Assumption) for Type 308 and 316 Stainless Steel Weld Metal as a Function of Pad Surface Preparation Technique (Measured on Bent Sample)

	308 (0.4 FN)		316 (0.4 FN)	
Surface Preparation	Ave. No.	Ave. Size, In.	Ave. No.	Ave. Size, In.
Milled	6	0.016	8	0.013
Surface Ground	44	0.008	17	0.009
Metallographically Polished	151	0.004	102	0.005

Brooks and Spruiell (Ref. 40) report that from dislocation densities present in 2½ in. (63.5 mm) thick Type 308 stainless steel weldments, the accumulated strain may be as high as 20%. One can easily visualize high strains in thick section weldments after once observing the extent of distortion evident if proper weld restraint is not utilized during welding. Suffice it to say that strains of 4% and greater always occur during welding of stainless steels and that the subsurface strains are much higher and may reach 20%.

Consider now the pad type specimens utilized for bend testing (Ref. 25). These "deposited on the surface" beads would naturally be less severely strained than those beads deposited in a groove in a heavy section weldment. In fact these test pads should represent the minimum restraint. The additional strain applied during bend testing may be equated to the additional strains occurring in thick section weldments (where fissures are observed). However, it should be recognized that all the additional strain in bend testing is

applied at room temperature whereas in a weldment the strains accumulate over a range of temperatures (any testing scheme suffers from some deficiencies). Nevertheless, the fissures observed in the bend specimens occur at the precise location and have the same appearance as those occurring in thick section weldments (Refs. 22, 23, 24). An almost unbelievable one-to-one correlation exists.

These observations strongly suggest that the same phenomena are occurring during pad production as occur in the heavy section weldments, save for a lesser total amount of strain accumulating in the pad. Thus, it appears that the fissures are present but tightly closed until the strain is applied during bend testing. Then and only then do they open sufficiently for detection.

If fissures in austenitic stainless steels are to be assessed as important in regard to mechanical properties, the "openness" of the fissures will not be an influential parameter. The size, shape, location and notch acuity are the truly important aspects. Thus whether a fissure is "tight" or "open" should not be important, and an incipient (unopened) fissure will be as important *(if important at all)* as one which is open and observable. In light of the influence of a fissure on the mechanical properties of austenitic stainless steel, it should be noted again that the fissures did not propagate during bend testing and, in fact, the ends of the fissures actually become blunted during deformation.

Fissure Surface Morphology and Energy Dispersive Analysis

To gain insight into the mechanism of fissure formation in austenitic stainless steels, the surfaces of the fissures in many weld metal types were examined utilizing the scanning electron microsope. In addition, energy dispersive X-ray analysis was performed on the fissure surfaces in an attempt to document segregation of certain elemental species. This examination technique and an indication of the useful information which can be obtained has been described by Lundin (Refs. 17, 31) and Honeycombe and Gooch (Refs. 18, 19, 41).

Honeycombe and Gooch (Ref. 18) claim to have documented three different fracture morphologies for Types 310 and 316 stainless steel:

1. A morphology which exhibited generally smooth features.
2. A morphology which showed dendritic films.
3. A morphology which showed a relatively featureless surface with many small particles on the surface.

Ludin (Refs. 17, 31) has observed morphology 1 in nickel, Type 310 stainless steel, X-750, TZM, molybdenum and Inconel 600, and he has observed morphology 3 in Inconel 600. Honeycombe and Gooch report that form 1 predominates and that forms 2 and 3 were less prevalent. This is in line with the observations of Lundin and the studies in this case for all the weld metals investigated.

In both morphologies 1 and 2, a liquid film plays a role in the cracking mechanism. In morphology 1 a single film generally covers the entire surface, while in morphology 2 the film may result from two different liquated phases. In all of the observations in this study, only one film type was noted.

The three SEM fractographs shown in Figs. 8a, 8b and 9 characterize the observations in this instance. Figures 8a and 8b show the predominant morphology at approximately X1000 and X2000 respectively. The pad surface can be seen in the upper and lower portions of Fig. 8a with the fissure surface extending across the central portion. The central portion only is shown in Fig. 8b. Note that the surface has a smooth appearance with a number of small holes and also protuberances extending upward from the surface.

All of these features suggest, as has been shown by others (Refs. 17, 18, 31), that a liquid film existed in this region at the time separation of the material occurred causing a fissure. The general shape of the cellular dendrites can be discerned (extending upwards in these micrographs). The protuberances extending upward from the surface result from the liquid metal necks that developed during separation with the liquid film present. The necked regions subsequently ruptured as the fissures opened. The features present on the surface defy explanation except for a liquid film hypothesis. Thus the fissures exposed during fissure bend testing originated at an elevated temperature and were not created during bending.

The fissure surface shown in Fig. 9 at X4500 is typical of only a small number of fissures, and it appears to be slightly different from those surfaces typified by Figs. 8a and 8b. Although it has relatively smooth features characteristic of the prior presence of liquid film, its features are somewhat finer. It is not considered to be associated with distinctly different mechanisms of fissure formation.

The fissure surfaces were analyzed using the energy dispersive X-ray mode of operation in the scanning electron microscope. As was anticipated and attested to by Honeycombe and Gooch (Ref. 18), only the major alloying elements, iron, nickel and chromium, and where appropriate molybdenum and columbium, were revealed. The SEM does not have the capability of detecting, even qualitatively, small amounts of trace elements on fracture surfaces, and it fluoresces the material to a considerable depth thus precluding elemental characterization of the remnants of the liquid film alone. Auger electron spectroscopy is perhaps an alternative approach to the problem although it is difficult to apply.

In summation, it is clear that a liquid film plays a dominant role in the fissure formation observed in all of the stainless steel weld metals studied. However, the elemental

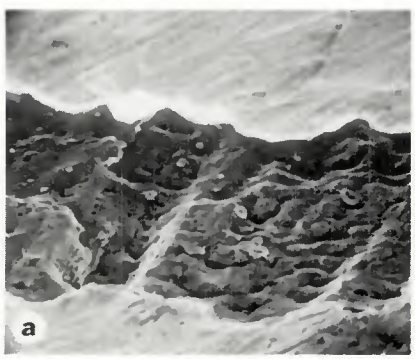

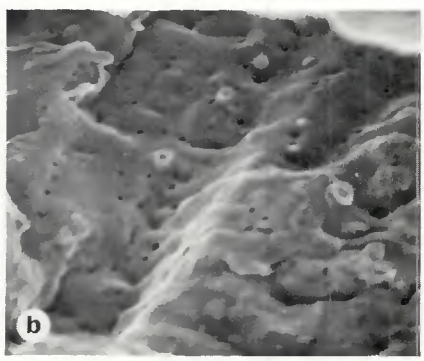

Fig. 8 — SEM micrograph showing the predominant type of fissure surface morphology. Left (a) — X1000; right (b) — X2000 (reduced 44% on reproduction)

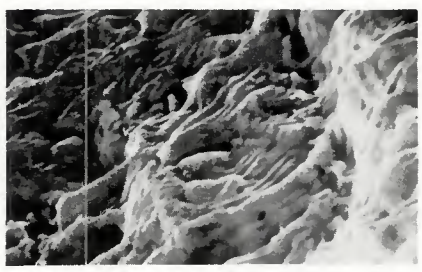

Fig. 9 — SEM micrograph of secondary fissure surface morphology. X4500 (reduced 46% on reproduction)

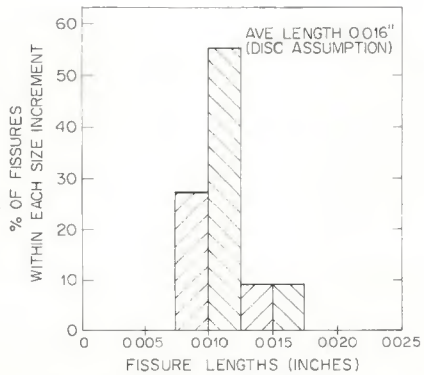

Fig. 10 — Fissure size distribution for Type 308 stainless steel weld metal (0.4 FN), milled surface, bend pad — 11 fissures measured

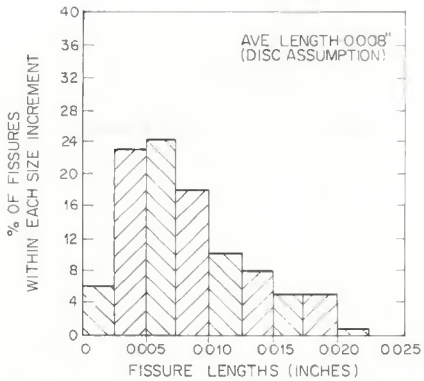

Fig. 11 — Fissure size distribution for Type 308 stainless steel weld metal (0.4 FN), ground surface, bent pad — 87 fissures measured

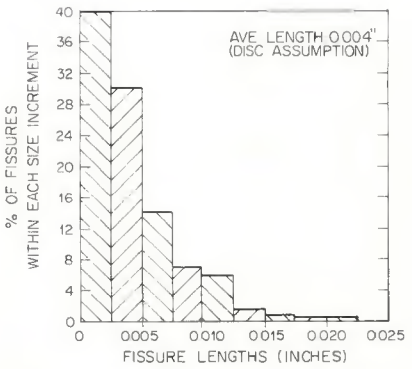

Fig. 12 — Fissure size distribution for Type 308 stainless steel weld metal (0.4 FN), polished and etched surface, bent pad — 302 fissures measured

species responsible for, or associated with, these films has not been revealed.

Fissure Sizes

The size of fissures present in austenitic stainless steel weld metals is of prime importance when considering their influence on the mechanical properties of weldments. This area of interest was discussed briefly in a previous article (Ref. 25) describing the early results in the overall study. It was also determined (Ref. 32) that the sizes of fissures revealed on the surfaces of the weld pad specimens was a direct function of the surface preparation technique and of the type of microscope and magnification used in the assessment.

The fissure size-preparation data are shown for Type 308 in Figs. 10-12. These figures will be useful in gaining an appreciation for the size distribution of the fissures and for illustrating how the "apparent" average fissure size varies with the ultimate resolution possible from the preparation and measurement techniques. In these figures the percentage of the total number of fissures observed within each 0.0025 in. (0.06 mm) size increment is shown. (Note that the total number of fissures observed varies for each surface preparation technique.) Three different surface preparation techniques were evaluated:

1. "Milled"-milling the surface and finishing with a 0.002 in. (0.05 mm) milling cut.

2. "Surface ground"-milling the pad surface followed by grinding with eight passes of 0.001 in. (0.025 mm) and finishing with four passes of 0.0005 in. (0.013 mm).

3. "Metallographically polished"-milling followed by grinding with eight passes of 0.001 in. (0.025 mm) and four passes of 0.0005 in. (0.013 mm) and finished by metallographically polishing the surface.

The fissure size distribution for the 11 fissures in two bent pads of Type 308 stainless steel weld metal (0.4 FN), surface prepared by the "milling" technique and examined at X40-X50, is shown in Fig. 10. Note that most of the fissures detected were approximately 0.010 to 0.012 in. (0.25 to 0.30 mm) long and that no fissure smaller than about 0.008 in. (0.20 mm) in length was detected. It is apparent that if fissures smaller than 0.008 in. (0.20 mm) are present, the surface roughness from milling prevented their detection. Also because of the high degree of surface roughness, examination of these pads at a magnification higher than X40-X50 was not possible optically nor practical in the SEM.

Fissures are considered to be present in the weld metal in approximately the shape of a disc, and thus the extent of a fissure exposed by surface preparation can vary from the full diameter of the disc to a very short segment of it. When a disc assumption is utilized, the average length of the fissures in the weld metal can be calculated from lengths of the fissures measured on the pad surface (Ref. 42). The average length of the fissures in the Type 308 stainless steel weld metal detected on the milled surface (Fig. 10) was calculated to be 0.016 in. (0.41 mm).

Figure 11 shows the fissure size distribution for the 87 fissures detected in two bent pads of Types 308 stainless steel weld metal (0.4 FN) finished by the "surface ground" technique and examined at X40-X50. Clearly the surface ground pad preparation technique reveals significantly more fissures (Ref. 87) than does milling (Ref. 11). Moreover, because the grinding technique causes less surface distortion, fissures smaller (as small as 0.002 in. or 0.05 mm in length) than those observed on the milled pads could be detected. It should be noted that the majority of the additional fissures detected are in the smaller size range (less than 0.010 in. or 0.25 mm in length). Utilizing the data from the ground pads, the average fissure length is calculated to be 0.008 in. (0.20 mm).

Table 2 — Influence of Thermal Cycling on Fissure Occurrence

	Area fissure density no./in.^{2}	Linear fissure density no./in.
Single HAZ cycle	8-17	2-4
Double HAZ cycle	95-120	19-24

Figure 12 presents the fissure size distribution for two bent pads of Type 308 stainless steel weld metal (0.4 FN) surface finished by metallographic polishing and etching and examined at X100-X200. Type 302 stainless steel fissures were detected in the two pads and it is to be noted that the majority of them were less than 0.005 in. (0.13 mm) in length. The calculated average length of the Type 302 fissures found in the metallographically polished and etched 308 weld pads was 0.004 in. (0.10 mm).

Quite obviously the smooth and well defined nature of the metallographically polished and etched pads, in conjunction with the high magnification at which they could be examined, permitted the detection of a large number of very small fissures. The number of larger fissures (greater than 0.010 in. or 0.25 mm in length) found in the metallographically polished pads compares favorably with the number (which are greater than 0.010 in. or 0.25 mm) found in the surface ground pads. In general, the larger fissures on the weld pad

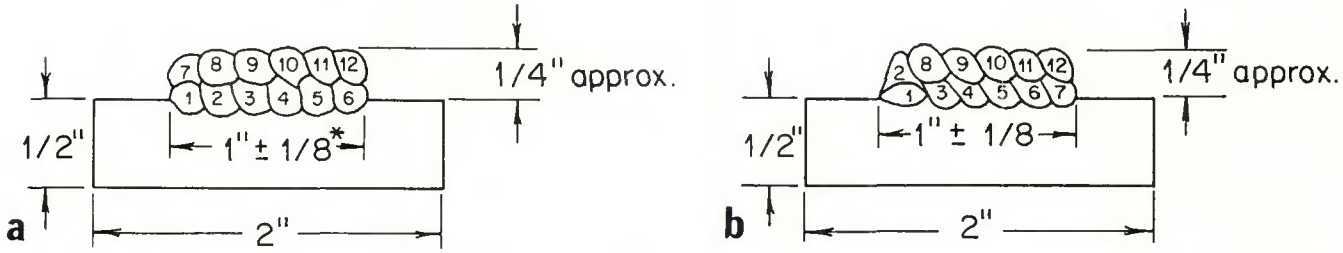

Fig. 13 — Weld pads cross-section showing bead sequence. Left (a) — recommended bead sequence; right (b) — alternate bead sequence resulting in two high peak temperature HAZ thermal cycles in bead 2*

surface can be detected by any of the three methods of surface preparation while most of the smaller fissures can be found only on metallographically polished pad surfaces.

The size distributions of fissures measured in the 316 weld metal pads finished by three different surface preparation methods can be compared to 308 by inspection of Table 1. It is to be noted that for both weld metal types (308 and 316), a similarity is evident in the size distribution when comparing corresponding surface preparation techniques.

16-8-2 weld metal was also evaluated using metallographically polished and etched pads. However only three fissures were detected, and thus the data were not amenable to either graphic presentation or the calculation of an average fissure size. The fissures found in the 16-8-2 material were 0.0015 to 0.0020 in. (0.04 to 0.05 mm) long and fall in the smallest size range of the Types 308 and 316 stainless steel weld metal.

By referring to Table 1, the above presentation may be summarized by noting that the apparent fissure size decreases as the surface preparation technique improves and the observation magnification and the resolution increase. The true average fissure size (disc assumption) is considered to be that determined from the polished pad data since it includes a statistically significant number and accounts for even the small fissures present. This yields an average fissure size of approximately 0.004-0.005 in. (0.10 to 0.13 mm) for Types 308 and 316 weld metal.

When comparing the average size for Type 316 stainless steel weld metal with those obtained from production fabricated heavy section Type 316 weldments, a significant difference is noted. The average size reported for actual weldments is approximately 0.014 in. (0.36 mm) (Ref. 22). (The ferrite levels for the tests reported here and the production weldments were about the same, ≈0.5 FN). The larger sizes in heavy section production weldments may be due to the fact that the strains accumulate at higher temperatures than in the room temperature bent pads and the degree of restraint may even impose higher total strains.

Weld pad must be within these limits to minimize variation in total pad surface area and variation in pad height.

The Influence of Thermal Cycling on Fissure Occurrence

In previous discussion it was emphasized that fissures occur only in the weld metal HAZs of subsequent weld passes. This was invariably true for the Fissure Bend Test pad studies (Refs. 25, 32) and those fissures studied by others (Refs. 22, 23, 24) in production weldments.

In the original fissure bend testing scheme, the top layer weld beads were deposited in sequence from one side of the pad to the other. This bead sequence is shown in Fig. 13a where beads 7-12 constitute the top layer and were deposited from left to right in the order shown. Thus bead 7 receives the high temperature thermal cycle effects from bead 8, and bead 8 is subjected to the same thermal cycles by bead 9, and so on with bead 12 being the only deposited upper layer bead not to be subsequently thermal cycled. Fissures were never found in bead 12 but only in the HAZ regions of beads 7-11, thus underscoring the weld metal HAZ fissuring phenomenon.

In follow-on investigations evaluating the Fissure Bend Test variables (Ref. 32) an altered weld pad bead sequence was fortuitously utilized for the Types 316, 308 and 16-8-2 stainless steel pads to be evaluated with metallographic preparation of the pad surface. This altered bead sequence is shown in Fig. 13b. Notice that bead 1 in the lower layer and bead 2, which forms a portion of the upper layer, were deposited before any other beads. Bead 3 caused bead 2 to experience a high temperature excursion and later bead 8 subjected bead 2 to a high temperature thermal history. Thus, bead 2 in the upper layer and in the final plane of examination was subjected twice to high temperature HAZ excursions. This was the only bead so influenced in the upper layers with the remainder experiencing only one high temperature HAZ excursion as described above.

For the specimens with the altered bead sequence, it became apparent that the majority of the fissures found were occurring in bead 2 (in the double HAZ produced by beads 3 and 8). The fissure count for the low ferrite pads (0.4 FN for 308 and 316, and 1.5 FN for 16-8-2) was treated so as to recognize this occurrence by computing the areal fissure density and the density along each interpass boundary (a linear density) for the single and double HAZ instances.

The areal density in the double HAZ region revealed approximately 95-120 fissures per square in., whereas for the single HAZ region the density was only 8-17 fissures per square in. The linear density (along the interpass boundary) was 19-24 fissures per in. of interpass for the double HAZ occurrence while it was 2-4 fissures per in. of interpass for the single HAZ. These data encompass both Types 308 and 316 weld metal with no clear distinction between the two. The 16-8-2 fissured an insignificant amount with only three fissures being found on two pads (8 sq. in., 40 in. of interpass). However, it is to be noted that the three fissures found were in the double HAZ region.

From this treatment (see Table 2) it was clear that the double HAZ occurrence is a significant factor in the fissuring tendency of 308, 316, and 16-8-2 weld metals at low ferrite levels. When the ferrite level for 316 was increased to 3.2 FN, fissures again occurred but only in the double HAZ region. For this pad there was a linear density of 3 fissures per in. of interpass (compared to approximately 20 fissures per in. at 0.4 FN) in the double HAZ region. However, for a Type 308 pad, at a nominal ferrite level of 2.5 FN, no fissures were found even in the interpass region of the bead subjected to the double HAZ thermal cycle. Additional testing has supported the fact that Type 316 weld

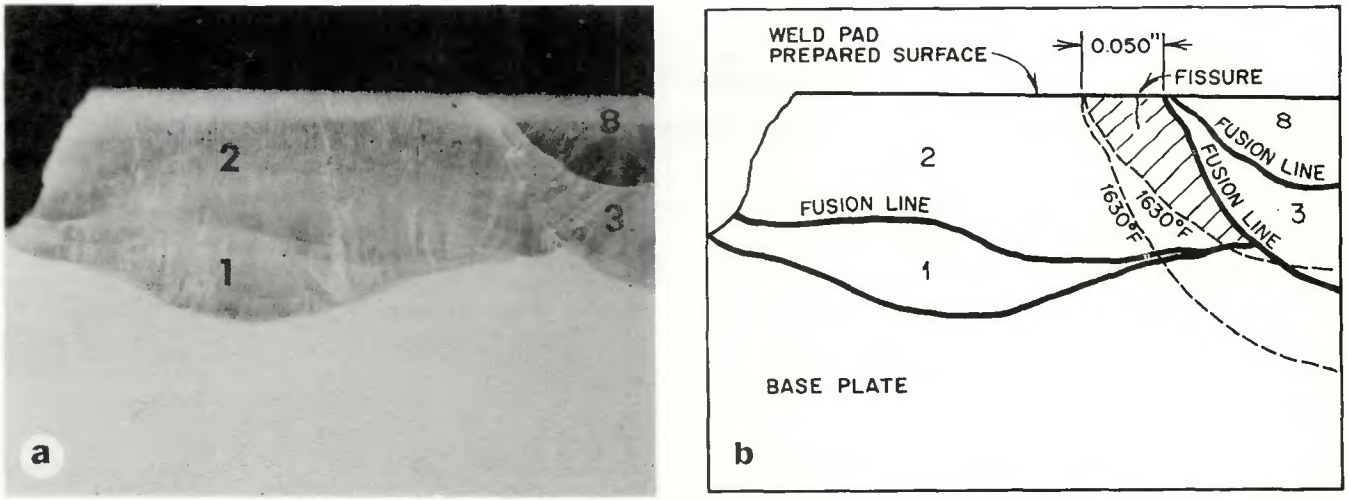

Fig. 14 — Portion of weld pad cross-section showing overlapping HAZ and its intersection with the prepared pad surface. Left (a) — light micrograph; right (b) — sketch. X12 (reduced 24% on reproduction)

metal at ferrite levels of 3.0 FN to 3.2 FN displays a low fissuring tendency in double HAZ regions, but that 308 weld metal at ferrite levels of 2.5 FN to 3.1 FN is insensitive to this occurrence. Thus double HAZ overlapping will be influencial in the determination of the minimum ferrite level to prevent fissuring.

To more clearly define the effect double HAZ thermal cycling has on fissuring tendency, a series of experiments was conducted utilizing a GTA remelt of surface ground SMA deposited pads. Both Types 316 and 308 stainless steel (0.6 FN) were utilized in the study. The GTA process was selected to remelt the SMA pads, because it produces a smooth flat bead with a well defined fusion line and is a quiescent process with minimal weld pool perturbation. Thus, it is easy to document the location of any fissure with regard to the weld fusion line.

The entire SMA pad surface was remelted by a series of overlapping GTA beads. Where double and triple HAZ experiences were desired, a given bead was refused two or three times thus producing double or triple HAZ experiences in the preceding bead. Care was exercised to control preheat and interpass temperatures in all cases to precisely maintain fusion line location. The energy input was varied from 6-60 kJ/in. (2.4×10^5 to 23.6×10^5 J/m) for individual weld pad studies, thus incorporating energy input as a variable. It is to be noted that the Ferrite Number was altered by the energy input variation. At low energy input, the Ferrite Number was 0.5 FN and with 60 kJ/in. (23.6×10^5 J/m) the Ferrite Number was 1.4 FN.

Regardless of the energy input for the GTA remelt studies, no fissures were found upon bend testing along interpass boundaries which were subjected to only a single HAZ experience. Only when a weld bead underwent double or triple HAZ experiences did any fissures appear upon bend testing, thus confirming the results of the directly deposited SMA weld bead studies.

Measurement of fissure locations from both the GTA and SMA pads were utilized to determine the exact region of the HAZ in which fissures occurred. These measurements for SMA beads showed that fissures were found in a region from the fusion line to approximately 0.050 in. (1.3 mm) from the fusion line. The fissures never crossed the interpass boundary and rarely extended to the interpass boundary. The majority of the fissures were found in a band 0.010 to 0.030 in. (0.25 to 0.76 mm) from the fusion line.

With the precise fissure location in the HAZ thus defined, it was now possible to determine the cracking temperature range by measuring the thermal distribution in the HAZ. This was accomplished for both the SMA and GTA weld beads utilizing the thermocouple implantation technique (Ref. 43). The welding conditions exactly duplicated the SMA (16 kJ/in. or 6.3×10^5 J/m) conditions. From these thermal measurements it was determined that a point 0.050 in. (1.3 mm) from the fusion line reached a peak temperature of approximately 1630 F, a point 0.030 (0.76 mm) reached a peak of 1950 F and a point 0.010 (0.25 mm) from the fusion line reached 2400 F (1316 C). Thus the overall HAZ temperature range in which the fissures were found extended from the bulk solidus (≈2650 F or 1454 C) to 1630 F (888 C) while the majority of the fissures fell in a range experiencing peak temperatures of 2400-1950 F (1316-1066 C).

The hot cracking temperature range for austenitic stainless steels was determined by Honeycombe and Gooch (Ref. 18), Shackleton (Ref. 12) and Senda *et al* (Ref. 2), using the Varestraint-thermocouple technique developed by Savage and Lundin (Ref. 44, 45). Shorshorov and Sokolov (Ref. 46) utilized an implanted thermocouple technique and Haddrill and Baker (Ref. 15) utilized a hot ductility apparatus for their determinations of the cracking range.

Those investigators utilizing the Varestraint technique record the hot cracking temperature range as extending from the bulk solidus to about 2300 F (1260 C) for a variety of austenitic stainless steel weld metals (GTA remelted). These data should be treated with caution especially at the high end of the range because Lundin (Ref. 47), utilizing high speed motion pictures showing Varestraint crack formation, has found that cracking initiates a short distance behind the instantaneous position of the solid-liquid interface and the cracks often propagate to the solid-liquid interface. (Cracks which propagate to the solid-liquid interface will always be coated with a liquid film.) Haddrill and Baker report a cracking temperature range of from 1650 to 1830 F (899 to 999 C) and Shorshorov and Sokolov report a range of 1740 F (949 C) to the bulk solidus.

The overall temperature range determined in this study (1630-2630 F or 888-1443 C) fits well with those of others. However, this study has shown that the majority of the fissures form at a temperature significantly below the bulk solidus in a range of 1950-2400 F (1066-1316 C).

By combining the information or observations as to the bead sequence in multipass welds and the data on the location of fissures and the temperature range over which they are most prone to occur, one can

better analyze the nature of fissuring in austenitic stainless steels. In regard to the Fissure Bend Test specimens in which the double HAZ cycling occurs, the influence of bead sequence can be clearly discerned by reference to Fig. 14.

The photomacrograph in Fig. 14a was obtained from a transverse section of an unbent 316 (0.4 FN) weld pad in which bead 2 experienced a double HAZ cycle from beads 3 and 8 (see Fig. 13b and associated discussion). The passes are numbered on the macrograph and the interpass boundaries can be clearly seen. The sketch in Fig. 14b (at the same scale as the macrograph) show the weld bead fusion lines and the 1630 F (888 C) peak temperature isotherms produced during the deposition of beads 3 and 8. Note that the cross-hatched region represents that area over which double HAZ (greater than 1630 F) thermal cycling has occurred. In this particular case a fissure exists in the center of the double HAZ region (it is difficult to see, however, at the magnification of the macrograph).

When the weld pad plane of examination passes through the double HAZ region, fissures may be found on the pad surface. However, when the weld pad plane of examination does not pass through the double HAZ region, the chance of finding fissures along the interpass exposed on the weld pad plane of examination is reduced.

Factors Contributing to the Multiple HAZ Thermal Cycle Phenomenon

The effect of multiple weld metal HAZ thermal cycles on the fissuring propensity of austenitic stainless steel weld metal is unmistakable in light of the foregoing discussions. This phenomenon appears to be the most influential element in the gamut of fissuring influences in austenitic stainless steels.

Since the occurrence of a single weld metal HAZ experience does not produce myriads of fissures upon the application of strain, it is clear that the strain tolerance of the grain boundary microstructural region is significantly reduced by multiple thermal cycling. This degradation of grain boundary ductility can be due to:

1. Enhanced segregation due to continued partitioning of harmful trace elements to the grain boundaries followed by liquation and rupture under strain.

2. Strengthening of the matrix by thermally-induced precipitate reactions, as is the case for some ductility-dip incidences. The increased strength of the matrix may cause strain accumulation in the degraded grain boundary microstructural region thus leading to rupture.

3. Strain-induced precipitation leading to a strengthened matrix and the subsequent accumulation of strain in the degraded microstructural region.

4. The simple accumulation of thermal and restraint strains over a range of temperatures produced by continued thermal cycling causing the strain tolerance of the grain boundary microstructural region to be exceeded.

Each of the elements above may play a role in the composite mechanism. Since the fissure morphology shows that liquation is virtually always associated with the occurrence of fissures, it must be a dominant factor. However, enhanced partitioning or segregation during the thermal cycles experienced after initial deposition should not be overlooked as contributory to the liquation.

Conclusions

1. The fissures observed in this study correlate with those found in production weldments with regard to location (along grain boundaries in ferrite-free areas in HAZs), and appearance. The size is somewhat smaller, however.

2. Fissures do not propagate with applied strain (up to 20% plastic strain), but rather the fissure tips become blunted as the bending strain increases.

3. The overall fissuring temperature range was defined as extending from the bulk solidus temperature to 1630 F (888 C) with the majority of the fissures forming in the 2400 to 1950 F (1316 to 1066 C) range.

4. Multiple HAZ thermal cycling plays a dominant role in fissuring of multipass austenitic stainless weldments.

5. The factors which lead to an enhanced fissuring propensity when multiple weld HAZ thermal cycles are imposed on previously deposited weld passes are:

(a) The accumulation of strain attendant upon multiple thermal cycling.

(b) Degradation of the strain tolerance of the metallurgical structure in and about a grain boundary by continued segregate partitioning or precipitation reactions.

(c) Liquation of the segregated grain boundary regions produced upon solidification and/or those boundaries with enhanced segregation produced during thermal cycling.

Acknowledgments

The authors acknowledge the sponsorship of the Welding Research Council, which provided a grant for the financial support through the auspices of the High Alloys Committee and the Stainless Steel Advisory Subcommittee. The program was conducted at the University of Tennessee and formed the basis of the Masters Thesis for Mr. D. F. Spond. Without the dedicated help of Mr. Ray Bellamy, who painstakingly prepared the specimens, this program could not have been completed. Mr. Michael Hunter contributed significantly on the SEM characterization and microanalysis of the discontinuities.

References

1. King, B. L., "Weld Metal and Heat Affected Zone Hot Cracking in Wrought Austenitic Stainless Steels," BWRA Report C 139/A/2/65, Feb. 1966.

2. Senda, T., *et al.*, "Fundamental Investigations on Solidification Crack Susceptibility for Weld Metal with Trans-Varestraint Test," *Welding Research Abroad,* Vol. 18 (6), 1972.

3. Masumoto, I., Tamaki, K. and Katsuna, M., "Hot Cracking of Austenitic Stainless Steel Weld Metal," *Journal of Japanese Welding Society,* Vol. 41 (11), 1972, Brutcher Trans. No. 8965.

4. Arata, Y., *et al.*, "Varestraint Test for Solidification Crack Susceptibility in Weld Metal of Austenitic Stainless Steels," *Trans. Japan Welding Research Institute,* Vol. 3 (1), 1974.

5. Poole, L. K., "The Incidence of Cracking in Weld Type 347 Steels," *Welding Journal,* 32 (8), Aug. 1953, Res. Suppl., 403-s to 412-s.

6. Puzak, P. P., Apblett, W. R., and Pellini, W. S., "Hot Cracking of Stainless Steel Weldments," *Welding Journal,* 35 (1), Jan. 1956, Res. Suppl., 9-s to 17-s.

7. Puzak, P. P., and Rischall, H., "Further Studies on Stainless Steel Hot Cracking," *Welding Journal,* 36 (2), Feb. 1957, Res. Suppl., 57-s to 61-s.

8. Fairchild, F. P., "Eight Years of Experience with Austenitic Steel Piping Materials at Elevated Steam Conditions," *Trans. of ASME,* Vol. 79 (8), 1957.

9. Curran, R. M., and Rankin, A. W., "Austenitic Steels in High Temperature Steam Piping," *Trans. of ASME,* Vol. 79 (8), 1957.

10. Younger, R. N., and Baker, R. G., "Heat Affected Zone Cracking in Welded High-Temperature Austenitic Steels," *Journal of Iron and Steel Institute,* Vol. 196 (10), 1960.

11. Christoffel, R. J., "Cracking in Type 347 Heat Affected Zone During Stress Relaxation," *Welding Journal,* 41 (6), June 1962, Res. Suppl., 251-s to 256-s.

12. Shackleton, D. N., "High Temperature Cracking Mechanism in the Heat Affected Zone of 25 Cr:20 Ni Stainless Steel Welds," BWRA Report M/47/69, Oct. 1969.

13. Rollason, E. C., and Bystram, M. C., "Hot Cracking of Austenitic Welds with Special Reference to 18/3/1 Cr-Ni-Nb Alloy," *Journal of Iron and Steel Institute,* Vol. 169 (12), 1951.

14. Cordea, J. N., Evans, R. M., and Martin, D. C., "Investigation to Determine

Causes of Fissuring in Stainless Steel and Nickel-Base Alloy Weld Metals," Technical Documentary Report No. ASD-TDR-62-317, Battelle Memorial Institute, June 1962.

15. Haddrill, D. M., and Baker, R. G., "Microcracking in Austenitic Weld Metal," *Brit. Welding Journal,* Vol. 13 (1), 1966.

16. Fredriks, H., and van der Toorn, L. J., "Hot Cracking in Austenitic Stainless Steel Weld Deposits," *Brit. Welding Journal,* Vol. 15 (4), 1968.

17. Lundin, C. D., "Welding Defects, Their Origin and Effect," II Interamerican Conference on Materials Technology, Mexico City, Mexico, Aug. 1970.

18. Honeycombe, J., and Gooch, T. G., "Microcracking in Fully Austenitic Stainless Steel Weld Metal," *Metal Construction and Brit. Welding Journal,* Vol. 2 (9), 1970.

19. Honeycombe, J., and Gooch, T. G., "Effect of Manganese on Cracking and Corrosion Behavior of Fully Austenitic Stainless Steel Weld Metals," *Metal Construction and Brit. Welding Journal,* Vol. 4 (12), 1972.

20. Honeycombe, J., and Gooch, T. G., "Microcracking in Fully Austenitic Stainless Steel Weld Metal," *Metal Construction and Brit. Welding Journal,* Vol. 7 (3), 1975.

21. Tamura, H., and Watanabe, T., "Mechanism of Liquidation Cracking in Weld Heat Affected Zone of Austenitic Stainless Steels," *Welding Research Abroad,* Vol. 20 (6), 1974.

22. Burghard, H. C., *et al.,* "An Investigation of the Properties of Type 316 Stainless Steel Weldments Containing Austenitic Microfissures," SWRI Topical Report No. 1, Project 17-3078, Aug. 15, 1971.

23. Buchhoit, R. D., *et al.,* "Laboratory Studies of Type 316 Stainless Steel Weld Metal from Maine Yankee Reactor Coolant System," Battelle Final Report, Sept. 17, 1971.

24. Thielsch, H., "Examination of Type 316 Stainless Steel Weld Deposit for Microfissuring and Delta Ferrite Contents for the Oconee Nuclear Power Station, Duke Power Company," Report No. 1057, Dec. 23, 1972.

25. Lundin, C. D., DeLong, W. T., and Spond, D. F., "Ferrite-Fissuring Relationship in Austenitic Stainless Steel Weld Metals," *Welding Journal,* 54 (8), Aug. 1975, Res. Suppl., 241-s to 246-s.

26. Truman, R. J., and Kirkby, H. W., "Some Ductility Aspects of 18-12-1 Nb Steel," *Journal of Iron and Steel Institute,* Vol. 196 (10), 1960.

27. Borland, J. C., and Younger, R. N., "Some Aspects of Cracking in Welded Cr-Ni Austenitic Steels," *Brit. Welding Journal,* Vol. 7 (1), 1960.

28. Borland, J. C., "Generalized Theory of Super-Solidus Cracking in Welds (and Castings)," *Brit. Welding Journal,* Vol. 7 (8), 1960.

29. Irvine, K. J., Murray, J. D., and Pickering, F. B., "The Effect of Heat-Treatment and Microstructure on the High Temperature Ductility of 18 Cr-12 Ni-1 Nb Steels," *Journal of Iron and Steel Institute,* Vol. 196 (10), 1960.

30. Hemsworth, B., *et al.,* "Classification and Definition of High Temperature Welding Cracks in Alloys," *Metal Construction and Brit. Welding Journal,* Vol. 1 (2), 1969.

31. Lundin, C. D., and Bennett, R. K., "Scanning Electron Microscopy of Fractures in Welded Structures," *IMS Proceedings,* 1971.

32. Lundin, C. D., DeLong, W. T., and Spond, D. F., "The Fissure Bend Test," submitted to *Welding Journal* for publication.

33. DeLong, W. T., "Ferrite in Austenitic Stainless Steel Weld Metal," *Welding Journal,* 53 (7), July 1974, Res. Suppl., 273-s to 286-s.

34. Gunia, R., and Ratz, G., "The Measurement of Delta Ferrite in Austenitic Stainless Steels," *WRC Bulletin No. 132,* Aug. 1968.

35. Stalmasek, E., "Measurement of Ferrite Content in Austenitic Stainless Steel Weld Metal Yielding Internationally Compatible Results," International Institute of Welding — Commission No. 2, "Arc Welding," Summary Report of Work Done by IIW Commission 2 in 1963-1973.

36. Goodwin, G., Cole, N., and Slaughter, G., "A Study of Ferrite Morphology in Austenitic Stainless Steel Weldments," *Welding Journal,* 51 (9), Sept. 1972, Res. Suppl., 425-s to 429-s.

37. Williams, N. T., *et al.,* "Stresses and Strains in Thick Austenitic Steel Plates During Welding," *Proceedings of the Second Commonwealth Welding Conference,* The Welding Institute, London, England, 1965.

38. Zhitnikov, N. P., and Zemzin, V. N., "Brittle Failure Tendency of Chromium-Nickel Steel Welds," *Svar. Proiz,* No. 10, 1970.

39. Shron, R. Z., "Influence of the Mechanical Heterogeneity of Welded Joints in Austenitic Steels on Their Susceptibility to Local Failure," *Svar. Proiz,* No. 4, 1965.

40. Brooks, C. R. and Spruiell, J. E., University of Tennessee, Private Communications, Aug. 1974.

41. Honeycombe, J., and Gooch, T. G., "Effect of Microcracks on Mechanical Properties of Austenitic Stainless-Steel Weld Metals," *Metal Construction and Brit. Welding Journal,* Vol. 5 (4), 1973.

42. DeHoff, R. T., and Rhines, F. N., *Quantitative Microscopy,* McGraw-Hill, New York, 1968.

43. Lundin, C. D., *et al.,* Unpublished research at University of Tennessee, May 1975.

44. Savage, W. F., and Lundin, C. D., "The Varestraint Test," *Welding Journal,* 44 (10), Oct. 1965, Res. Suppl., 443-s to 442-s.

45. Savage, W. F., and Lundin, C. D., "Application of the Varestraint Technique to the Study of Weldability," *Welding Journal,* 45 (11), Nov. 1966, Res. Suppl., 497-s to 503-s.

46. Shorshorov, N. K., and Sokolov, Y. V., "The Temperature Range in Which Hot Cracks Develop When Single Phase Nickel Alloys are Fusion Welded," *Avtom. Svarka,* Vol. 16 (4), 1963.

47. Lundin, C. D., Unpublished research at Rensselaer Polytechnic Institute, 1968.

WRC Bulletin No. 219

"Experimental Investigation of Limit Loads of Nozzles in Cylindrical Vessels"
by Fernand Ellyin

Experimental results of elastic-plastic behavior and plastic limit loads (yield point loads) of five tee-shaped cylinder-cylinder intersections and a plain pipe are reported herein. The intersecting models were machined from a single hot-rolled steel plate. The nozzle-vessel attachments (or branch-pipe tee connections) were subjected to one of the loading modes: internal pressure, in-plane or out-of-plane couples applied to the nozzle extremity. The out-of-plane couple loading is found to be the critical case.

* * *

Publication of this report was sponsored by the Pressure Vessel Research Committee of the Welding Research Council.

The price of WRC Bulletin 219 is *$6.00 per copy.* Orders should be sent with payment to the Welding Research Council, United Engineering Center, 345 East 47th St., New York, N.Y. 10017.